Subwavelength structures for taper waveguides

Subwavelength structures for taper waveguides

Paulo Lourenço[*1,2], Alessandro Fantoni[1,2], João Costa[1,2], Miguel Fernandes[1,2], Manuela Vieira[1,2]

[1] DEETC-ISEL-Instituto Politécnico de Lisboa, 1949-014 Lisboa, Portugal
[2] CTS-UNINOVA, Caparica, Portugal

[*] pj.lourenco@campus.fct.unl.pt

Abstract. In Photonic Integrated Circuits (PICs) it is often necessary some sort of mismatch adaptation between waveguides of different cross-sections. There are several instances of such a designing constraint, being the vertical coupling between the PIC and an optical fibre probably the most representative of all examples. Here, the beam of electromagnetic energy inside the PIC must be inserted/extracted through/to an optical fibre. Typical core diameters are approximately 10 µm and 5 µm, for single mode optical fibres operating in the near infrared and visible wavelengths, respectively. On the other hand, the optical interconnects linking individual structures in PICs are usually single mode waveguides, 400 to 500 nm wide and a few hundreds of nanometres thick. This presents a bidimensional mismatch between the optical fibre and the single mode waveguide within the PIC, that requires both lateral and longitudinal beam expansions. In this work, we have approached the lateral expansion of the fundamental mode propagating in a single mode waveguide, at the operating wavelength of 1550 nm and being coupled out into an optical fibre, through a grating structure 14.27 µm wide. To this end, we have designed and simulated a subwavelength metamaterial planar structure, which is able to expand laterally the fundamental mode's profile from 450 nm to 14.27 µm, within 11.1 µm. Furthermore, we will be presenting the results obtained when comparing this structure with several linear inverted taper waveguides, regarding coupling and propagation efficiencies. Namely, we compared the coupling efficiencies of the modes propagating in an 100 µm long waveguide, when being excited by the analytically calculated fundamental mode and the fields obtained at the end of the designed structure. The results obtained for the designed structure 11.1 µm long and the calculated fundamental mode showed a coupling efficiency of -1.53 dB and -1.20 dB, respectively.

1. Introduction

In photonic integrated circuits it is often necessary a structure to compensate for the cross-section mismatch between waveguides of different dimensions. One of the most representative instances of such a constraint is the vertical outcoupling of light, often used between an optical fibre and a photonic integrated chip. The Electromagnetic (EM) beam of energy diffracted by a resonant waveguide grating propagates in free space and towards a single mode optical fibre, where it couples with its fundamental mode. This grating structure must be wide enough to assure efficient coupling with the beam of energy of the optical fibre. Typical core widths are approximately 10 µm and 5 µm for single mode optical fibres operating in the near infrared and visible wavelengths, respectively. Thus, these grating structures must be wider to couple the fundamental mode of the resonant waveguide grating with the diffracted EM energy beam, which is coupling to the lowest order mode of the optical fibre.

Furthermore, the optical interconnects linking operational structures in the photonic integrated circuit are usually single mode waveguides, 400 to 500 nm wide. Thus, a spot-size conversion is necessary between the single mode waveguide and the resonant waveguide grating mode profiles. Often, a taper waveguide performs the lateral expansion of the propagating mode and provides mode profile matching between narrow and wider waveguides. Once the lateral expansion of the mode profile occurs efficiently (no losses), we get adiabatic transfer of energy between the different cross-section waveguides, and the only mode propagating in the wider structure is the fundamental one.

Back in 1977, Burns et al. [1] have presented the general derivation of equations to guide the design of adiabatic waveguide tapers while minimizing their length. The derived main rule of adiabatic taper design is governed by the following equation:

$$\theta < \frac{\lambda_0}{2Wn_{eff}} \tag{1}$$

here, θ is the local half angle at a given z point along the taper, λ_0 is the free space wavelength, W is the width of the taper at a given z location and n_{eff} is the modal index of the propagating mode in the taper. Moreover, the half slope of a linear taper (or a linear section of a taper) is given by:

$$\tan\left(\frac{\alpha}{2}\right) = \frac{W_{high} - W_{low}}{2L} \tag{2}$$

where, α is the sum of left and right sidewall angles (assuming a symmetric taper), W_{high} and W_{low} are the waveguides wider and narrower widths, respectively, and L is the length of the taper waveguide. Previous work [1] reported an adiabatic parabolic taper waveguide (reduced to three linear segments to facilitate fabrication) connecting 30 μm and 4 μm wide waveguides, only through a taper over 2 mm long. Nonetheless, parabolic tapers are not the only solutions for adiabatic coupling. There are other configurations also capable of highly efficient transfer of EM energy between different cross-section waveguides. Namely, one may find reports in the literature of adiabatic exponential, gaussian and linear taper waveguides. Nevertheless, they all require long tapered waveguides and shallow slopes of the sidewalls.

More recently, research has been developed on a different taper configuration – the denominated non-adiabatic tapers. Examples of such configurations have been reported by Spühler [2] and Luyssaert [3] which, by exploiting the developments in genetic algorithms, have announced highly efficient and compact non-adiabatic taper waveguides. Also, Zhang [4] and Liu [5] used a similar strategy to design their compact tapers. The former exploited the effective medium theory to design a row of inclusions of a different refractive index material, to converge the EM beam through a linear taper and into a focal point, and the latter, by placing identical inclusions along the sides and in the core of the taper waveguide, obtained a staircase-like taper with perturbations of the core refractive index at locations calculated by an evolutionary algorithm. Finally, Huang [6] has exploited the Graded Index (GRIN) concept by designing a structure that consisted of several layers of alternating materials with different thicknesses, creating a material with a parabolic refractive index profile along the height of the structure. Our proposed line of action considers a similar approach, only creating a specific refractive index profile through the width of the structure instead of along its thickness.

This work bases its approach on the GRIN concept to design an inverted taper waveguide, at the operating wavelength of 1550 nm. The engineered structure consists of a planar metamaterial waveguide, which is able to expand laterally the propagating mode's profile from 450 nm to 14.27 μm (typical width of the resonant waveguide grating), within an 11.1 μm long structure. The metamaterial structure is formed by a Hydrogenated Amorphous Silicon (a-Si:H) waveguide, 250 nm thick and 14.27 μm wide. This waveguide has been virtually divided in 51 segments of equal width and, in each of them, we have placed a number of Silicon Dioxide (SiO_2) cylindrical inclusions of subwavelength dimensions to define the refractive index profile as required by the tapering functionality. When subwavelength

periodic perturbations are involved, the effective medium approximation may be used to calculate the effective refractive index of the resulting material through the following equation [7]:

$$\frac{n_{eff}^2}{n_{core}^2} = \frac{n_{hole}^2(1+f) + n_{core}^2(1-f)}{n_{hole}^2(1-f) + n_{core}^2(1+f)} \quad (3)$$

where n_{eff} is the effective refractive index, n_{hole} is the refractive index of the cylindrical perturbation, n_{core} is the refractive index of the waveguide and f is the filling factor. From equation 3, one can calculate the effective refractive index of the medium, once all the other variables are known. Or, if the intended effective refractive index is known, one may calculate the filling factor. On the other hand, the filling factor of a hexagonal lattice of cylindrical inclusions of *D* diameter, embedded in a waveguide of d width and lattice constant $a = 2/3\,d$, may be calculated through equation 4 [8], and enabled the design of the metamaterial waveguide with an engineered gaussian profile for the refractive index [9]:

$$f = \frac{3\pi D^2}{\sqrt{3}da} \quad (4)$$

2. Methods

The development of the presented structures has been accomplished through RSoft [10], a photonic tools software platform for the design, simulation, analysis and optimization of arbitrary optical structures. In this work, we have used the software packages implementing the beam propagation method [11] and the finite differences time domain algorithm [12], for the simulation and performance analysis of the designed structures. The beam propagation method has been employed to evaluate the propagation in longer structures and where reflections are of no significance (inverted taper and wider section waveguide), and the finite differences time domain algorithm was utilized to analyse the propagation/reflection through/at complex structures (planar metamaterial waveguide) and interfaces between materials.

In our simulations, we have considered an identical Silicon-on-Insulator (SOI) platform for both the linear inverted taper and the planar metamaterial waveguides. This platform consists of, from bottom to top, a semi-infinite layer of Silicon (Si), a SiO_2 layer 2 µm thick and where the 250 nm high a-Si:H taper waveguides are designed as deposited halfway upwards the SiO_2 height, and a semi-infinite layer of air. Figure *1* presents a 3D representation and a Z plane cut of the refractive index of these structures, respectively on both left and right sides of a) and b) images.

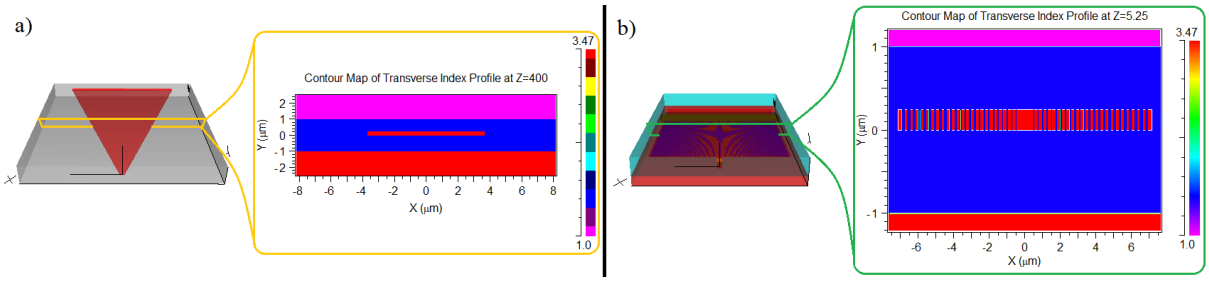

Figure 1 - a) 3D representation and cut plane at Z=400 um of the linear taper; b) 3D representation and cut plane at Z=5.25 µm of the planar metamaterial waveguide.

The linear inverted taper waveguide has been evaluated regarding its coupling efficiency for a range of representative structure lengths, namely 150 µm, 200 µm, 250 µm and 300 µm, as the first set of iterations, and 400 µm, 550 µm, 700 µm, 850 µm and 1000 µm, for the second set. The coupling efficiency has been determined by launching the fundamental Transverse Electric (TE) mode of the narrower cross-section (250 nm x 450 nm) and monitor the overlap integral as it couples to the fundamental mode of the wider cross-section (250 nm x 14.27 µm). Simultaneously, we monitor the total power propagating in the inverted taper waveguide. Figure *2* depicts (on the left and right, respectively) the lateral field expansion as propagation evolves throughout the structure for the 850 µm

long inverted taper waveguide and the coupling efficiency results obtained for the first and second sets of iterations.

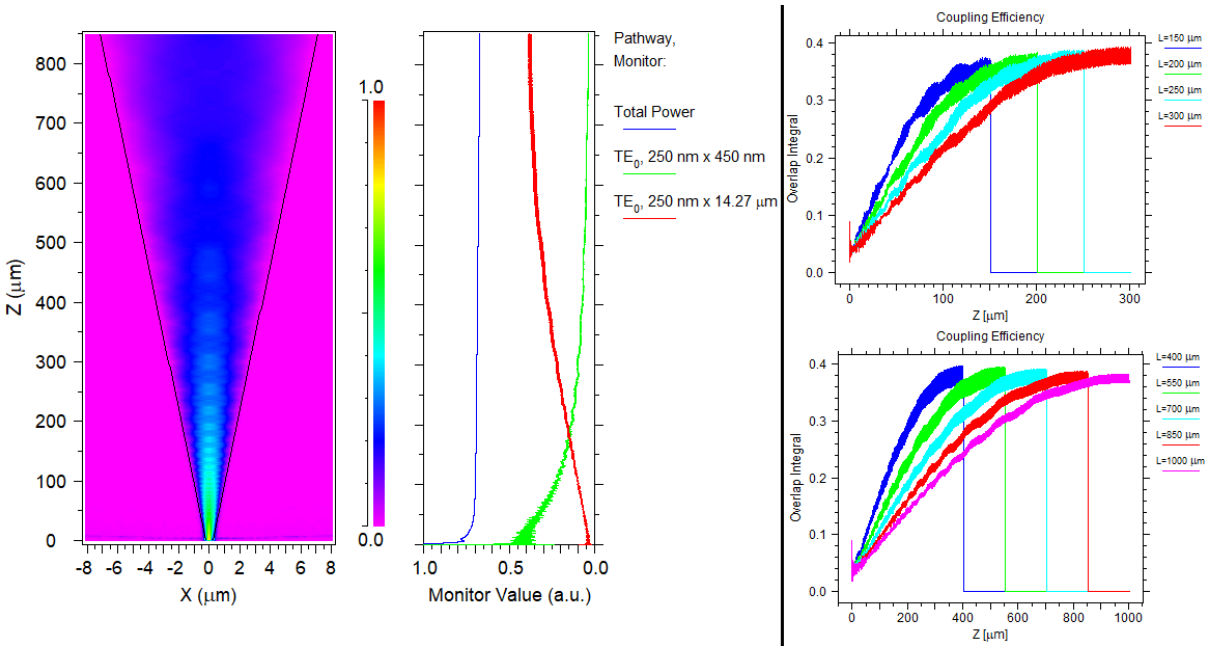

Figure 2 - (left): fields propagation along the 850 µm instance of the linear taper waveguide; graph shows the coupling/decoupling evolution of the fields with the fundamental mode of the wider/narrower cross section. (right): coupling efficiency obtained for the inverted taper waveguide.

Next, we evaluated the performance of the planar taper waveguide by launching the fundamental mode at the input waveguide (cross-section 250 nm x 450 nm), while monitoring the mode's propagation throughout the structure and assessing the coupling efficiency through the overlap integral to the fundamental mode of the wider cross-section waveguide (250 nm x 14.27 µm). Figure 3 shows the propagation of the fields along the structure and the obtained coupling efficiency.

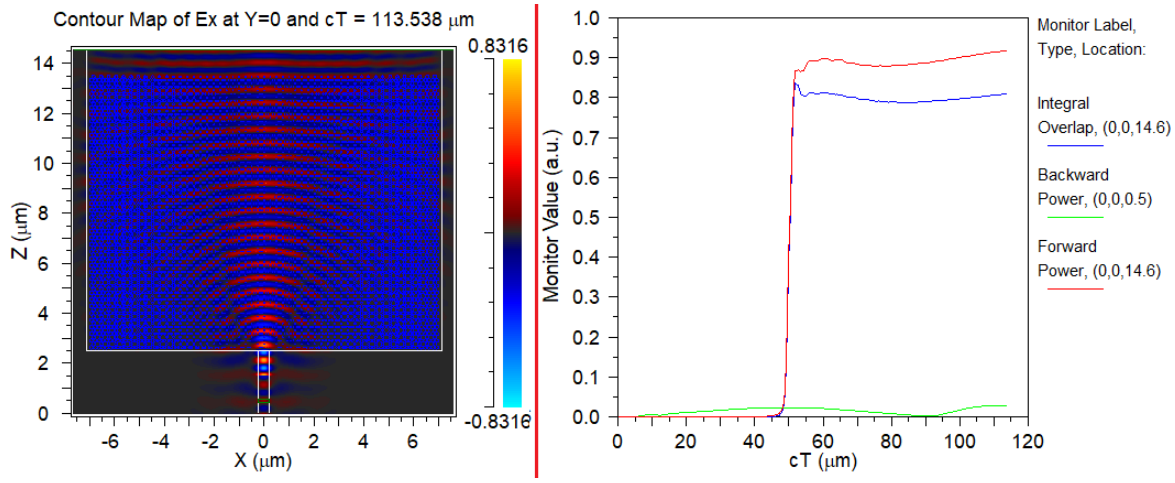

Figure 3 - (left): propagation of the fields throughout the structure; (right): integral overlap over the TE0 mode of the wider cross section waveguide at the end of propagation.

3. Results

The coupling efficiency data of the linear inverted taper waveguide was curve approximated through a moving least squares fit, for interpretation purposes.

Figure 4 - Moving least squares fit; a) iterated lengths 150 to 300 µm; b) iterated lengths 400 to 1000 µm.

shows the graphs obtained for all iterated instances of the structure and the best result is the 550 µm long taper, with a coupling efficiency of -1.19 dB. All the iterated lengths have presented the following results: - [150 µm <> -1.51 dB]; [200 µm <> -1.39 dB]; [250 µm <> -1.28 dB]; [300 µm <> -1.22 dB]; [400 µm <> -1.21 dB]; [550 µm <> -1.19 dB]; [700 µm <> -1.21 dB]; [850 µm <> -1.23 dB]; [1000 µm <> -1.27 dB].

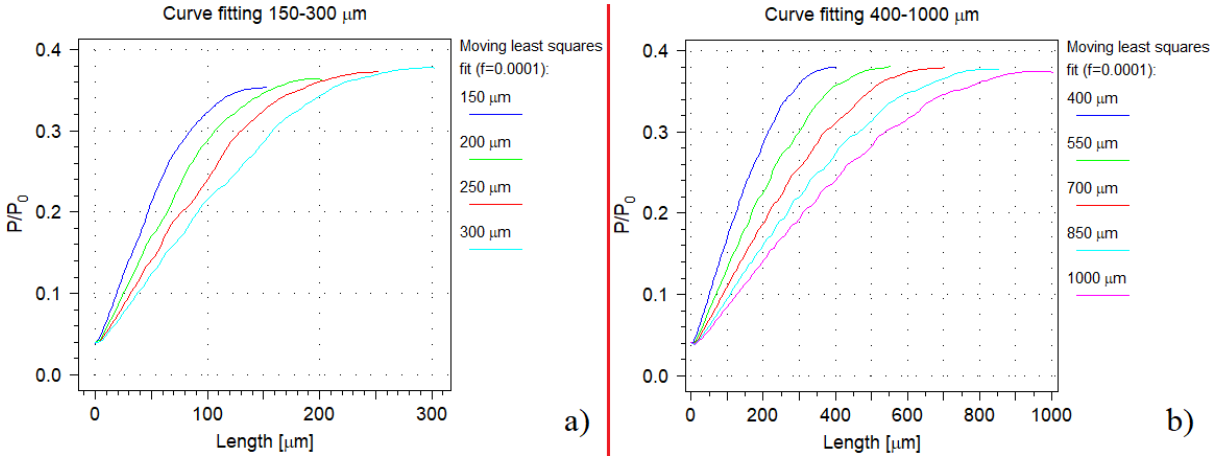

Figure 4 - Moving least squares fit; a) iterated lengths 150 to 300 µm; b) iterated lengths 400 to 1000 µm.

Regarding the planar taper waveguide, the results obtained for the propagated fields and the fundamental mode of the wider cross-section revealed a coupling efficiency of -0.92 dB, which is better than any of the simulated linear taper waveguides. Anyhow, the obtained fields were propagated through a waveguide 100 µm long and compared with the propagation of the fundamental mode under the same conditions, the former revealing a lower coupling efficiency of 0.55 dB when compared to the latter, as depicted in Figure 5.

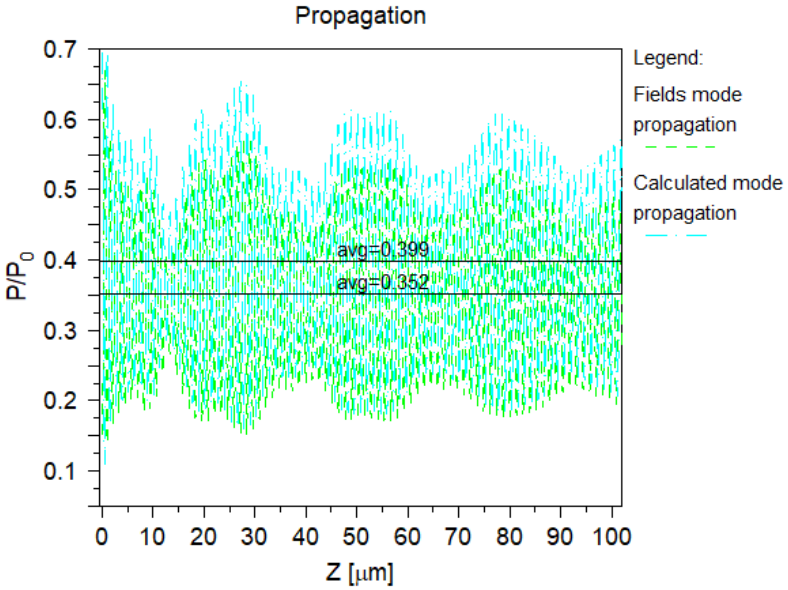

Figure 5 - Propagation of the fields obtained at the planar taper waveguide and the fundamental mode of the wider waveguide.

4. Conclusions

In this work we propose an alternative approach for the lateral expansion of a propagating fundamental mode. By using a planar taper waveguide consisting of a metamaterial structure, we were able to expand

laterally the TE_0 mode from 450 nm to 14.27 μm in a waveguide 11.1 μm long, resulting in an integral overlap penalty of 0.55 dB, when assuming as reference the calculated TE_0 mode and, as arbitrary propagation length, a 100 μm a-Si:H waveguide embedded in SiO_2. Considering the obtained results for both, the best case scenario of length iterations ranging 150 μm to 1000 μm, the 400 μm long taper has achieved a coupling efficiency of -1.20 dB, and the 11.1 μm long planar taper waveguide has shown -1.53 dB for the same metric. Moreover, and analysing the results obtained at the other length iterations, we realize that the planar taper waveguide presents lower coupling efficiency than all the other instances, although not significant.

Given the differences in magnitude for the coupling efficiencies obtained in our proposed planar taper waveguide, we have concluded that our metamaterial based structure shows similar performance when compared with the linear inverted taper and may present itself as an alternative for the latter structure. Moreover, the reported coupling efficiency resulted of lateral expansion (from 450 nm to 14.27 μm) of the mode profile in a metamaterial planar waveguide 11.1 μm long, while a typical linear inverted taper waveguide requires several hundreds of micrometres.

Acknowledgements
This research has been supported by EU funds through the FEDER European Regional Development Fund and by Portuguese national funds by FCT – Fundação para a Ciência e a Tecnologia through grant SFRH/BD/144833/2019, and projects IPL/2021/MuMIAS-2D/ISEL and IPL/2021/wavesensor_ISEL.

References

[1] W. K. Burns, A. F. Milton, and A. B. Lee, “Optical waveguide parabolic coupling horns,” *Appl. Phys. Lett.*, vol. 30, no. 1, pp. 28–30, 1977, doi: 10.1063/1.89199.
[2] M. M. Spuhler, B. J. Offrein, G.-L. Bona, R. Germann, I. Massarek, and D. Erni, “A very short planar silica spot-size converter using a nonperiodic segmented waveguide,” *J. Light. Technol.*, vol. 16, no. 9, pp. 1680–1685, 1998, doi: 10.1109/50.712252.
[3] B. Luyssaert, P. Bienstman, P. Vandersteegen, P. Dumon, and R. Baets, “Efficient nonadiabatic planar waveguide tapers,” *J. Light. Technol.*, vol. 23, no. 8, pp. 2462–2468, 2005, doi: 10.1109/JLT.2005.850795.
[4] J. Zhang, J. Yang, H. Xin, J. Huang, D. Chen, and Z. Zhaojian, “Ultrashort and efficient adiabatic waveguide taper based on thin flat focusing lenses,” *Opt. Express*, vol. 25, no. 17, p. 19894, 2017, doi: 10.1364/oe.25.019894.
[5] Y. Liu *et al.*, “Adiabatic and Ultracompact Waveguide Tapers Based on Digital Metamaterials,” *IEEE J. Sel. Top. Quantum Electron.*, vol. 25, no. 3, 2018, doi: 10.1109/JSTQE.2018.2846046.
[6] Y. Huang and S.-T. Ho, “Superhigh numerical aperture (NA>15) micro gradient-index lens based on a dual-material approach,” *Opt. Lett.*, vol. 30, no. 11, p. 1291, Jun. 2005, doi: 10.1364/OL.30.001291.
[7] D. Gao and Z. Zhou, “Nonlinear equation method for band structure calculations of photonic crystal slabs,” *Appl. Phys. Lett.*, vol. 88, no. 16, p. 163105, Apr. 2006, doi: 10.1063/1.2194887.
[8] Y. Ding, H. Ou, and C. Peucheret, “Ultrahigh-efficiency apodized grating coupler using fully etched photonic crystals,” *Opt. Lett.*, vol. 38, no. 15, p. 2732, Aug. 2013, doi: 10.1364/OL.38.002732.
[9] P. Lourenço, A. Fantoni, J. Costa, M. Fernandes, and M. Vieira, “Metamaterials in waveguide to fiber couplers,” in *Physics and Simulation of Optoelectronic Devices XXX*, Mar. 2022, vol. 1199509, no. March, p. 13, doi: 10.1117/12.2610335.
[10] RSoft, “Synopsys RSoft Solutions.” https://www.synopsys.com/optical-solutions/rsoft.html (accessed Jul. 10, 2021).
[11] BeamPROP, “BeamPROP - Synopsys.” https://www.synopsys.com/photonic-solutions/rsoft-photonic-device-tools/passive-device-beamprop.html (accessed Mar. 04, 2020).

[12] FullWAVE, “FullWAVE - Synopsys.” https://www.synopsys.com/photonic-solutions/rsoft-photonic-device-tools/passive-device-fullwave.html (accessed Dec. 29, 2019).